

## Supporting Information

### Microstructurally Engineered Nanocrystalline Fe-Sn-Sb Anode: Towards Stable High Energy Density Sodium-ion Batteries

Eldho Edison,<sup>a</sup> Sivaramapanicker Sreejith,\*<sup>b</sup> Hao Ren,<sup>a</sup> Chwee Teck Lim \*<sup>b,c</sup> and Srinivasan Madhavi \*<sup>a</sup>

---

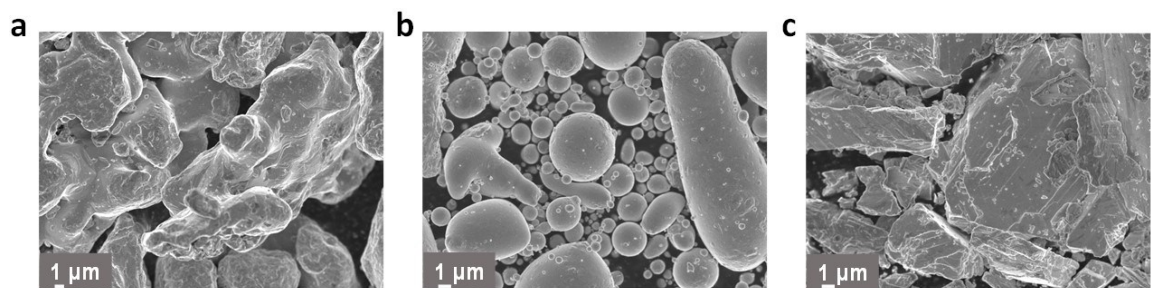
<sup>a.</sup> School of Materials Science and Engineering, Nanyang Technological University, 50 Nanyang Avenue, 639798, Singapore. Email: [madhavi@ntu.edu.sg](mailto:madhavi@ntu.edu.sg)

<sup>b.</sup> Biomedical Institute for Global Health Research and Technology, National University of Singapore, 117599, Singapore. Email: [bigsiv@nus.edu.sg](mailto:bigsiv@nus.edu.sg) ; [sreejith.siva@gmail.com](mailto:sreejith.siva@gmail.com)

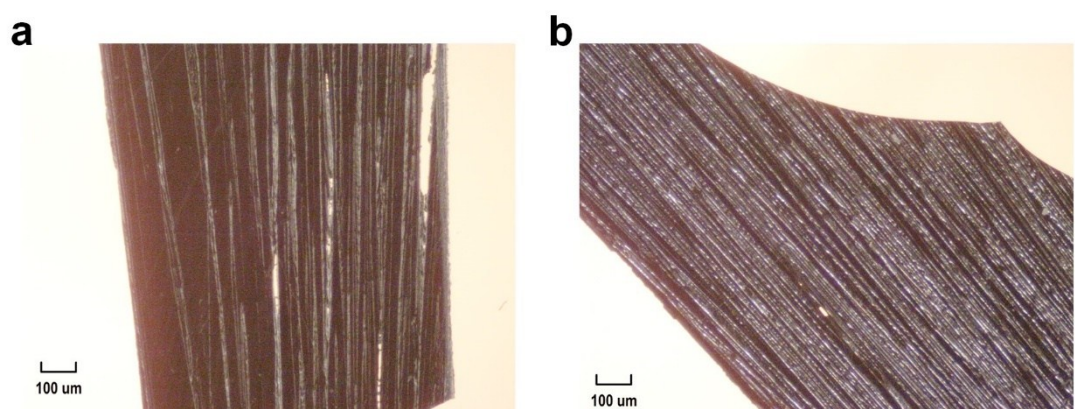
<sup>c.</sup> Department of Biomedical Engineering, National University of Singapore, 2 Engineering Drive 3, 117581, Singapore. Email: [ctlim@nus.edu.sg](mailto:ctlim@nus.edu.sg)

## Table of Contents

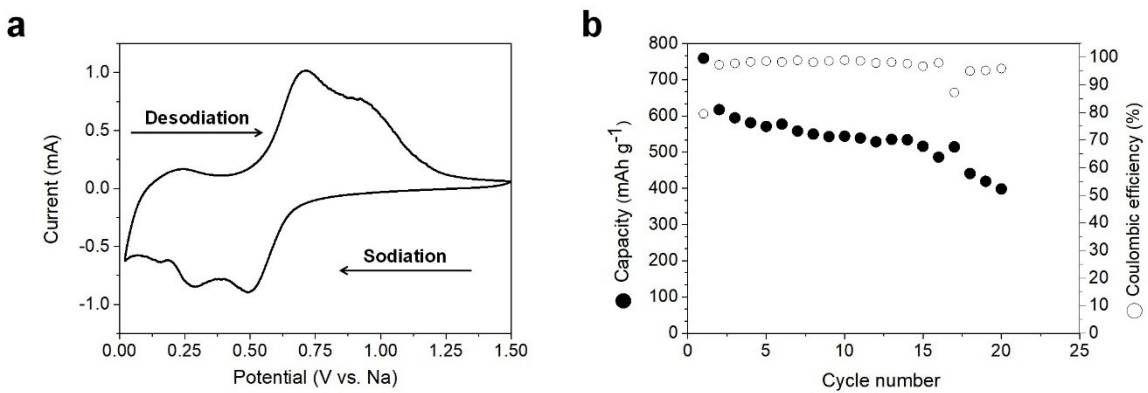
Item	Page no.
<b>Figure S1</b>	S-3
<b>Figure S2</b>	S-3
<b>Figure S3</b>	S-4
<b>Figure S4</b>	S-4
<b>Figure S5</b>	S-5
<b>Figure S6</b>	S-5
<b>Figure S7</b>	S-6
<b>Figure S8</b>	S-6
<b>Figure S9</b>	S-7
<b>Figure S10</b>	S-8
<b>Figure S11</b>	S-9
<b>Figure S12</b>	S-9
<b>Table S1</b>	S-10
<b>Table S2</b>	S-10
<b>References</b>	S-11



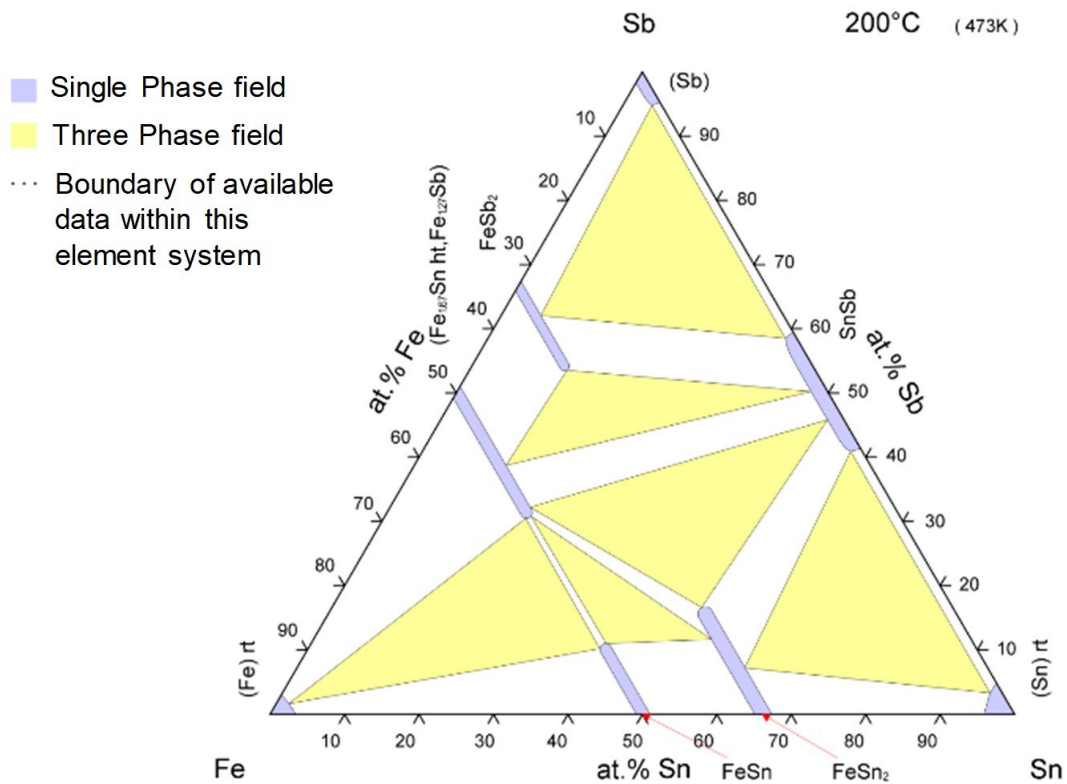
**Figure S1.** Metal powders used as precursor for the rapid solidification process. a) Fe powder. b) Sn powder. c) Sb powder.



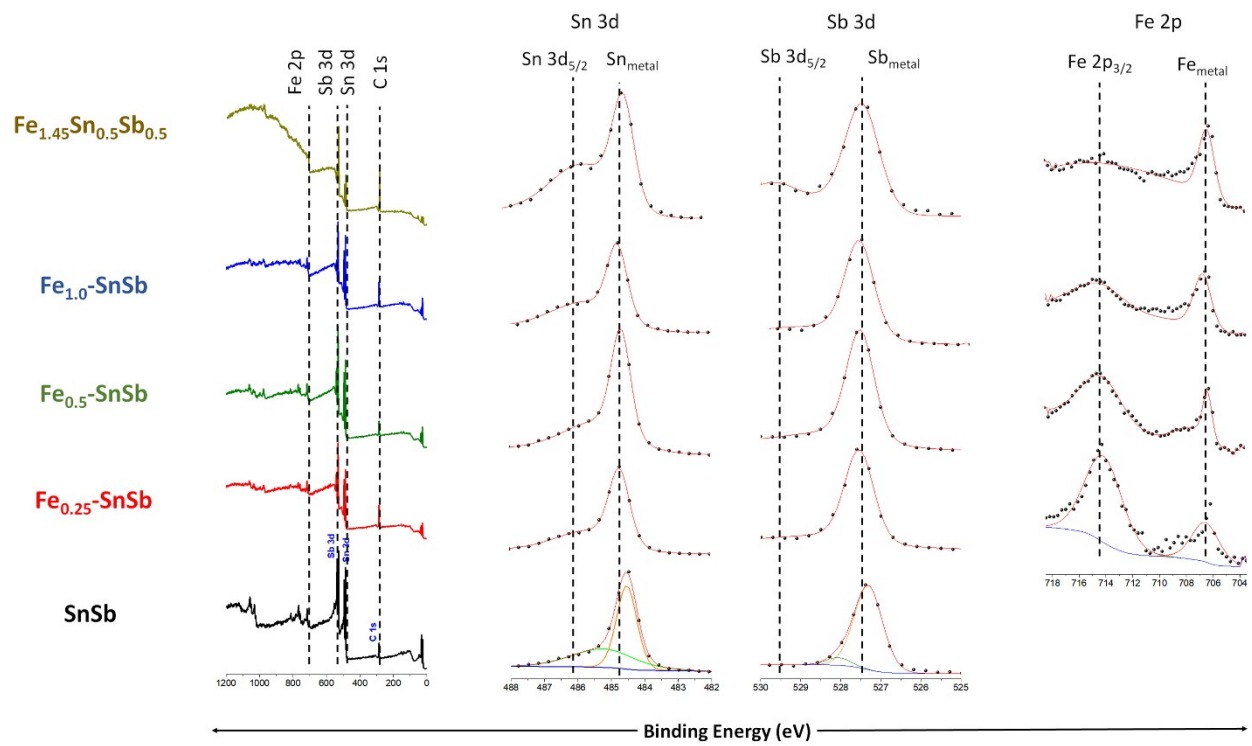
**Figure S2.** Optical microscopy images of the rapidly solidified ribbons of a) SnSb and b)  $\text{Fe}_{1.0}\text{-SnSb}$ .



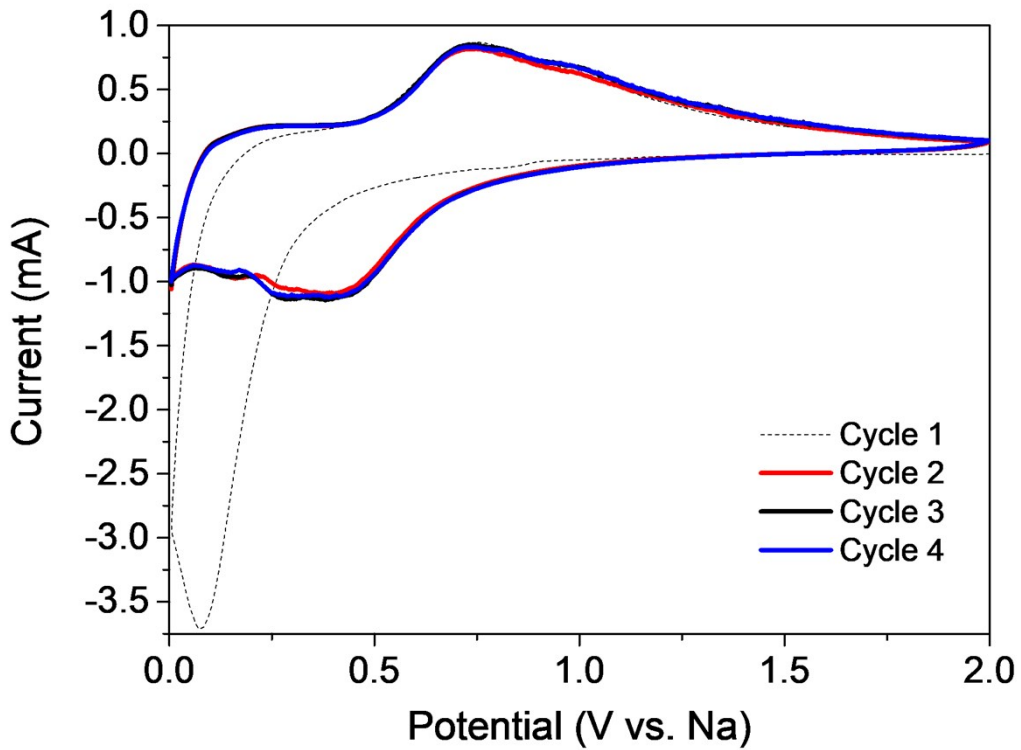
**Figure S3.** Electrochemical performance of SnSb anode. a) Cyclic voltammogram at  $0.1 \text{ mV s}^{-1}$  and b) Galvanostatic charge-discharge test at  $50 \text{ mA g}^{-1}$  in the potential window  $0.005 - 2 \text{ V}$  vs. Na.



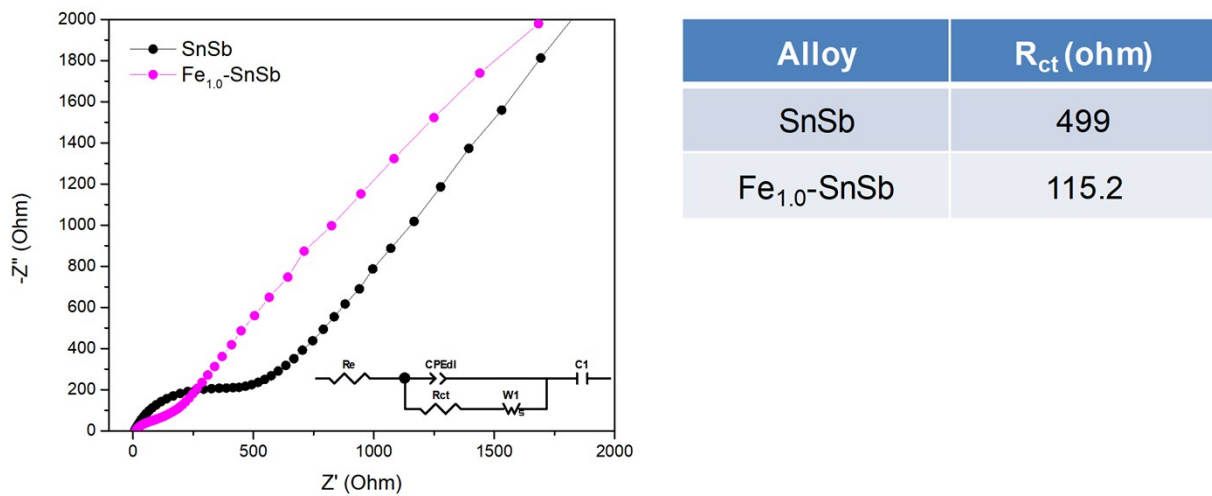
**Figure S4.** Fe-Sb-Sn isothermal section of ternary phase diagram.<sup>1</sup> ©Springer & Material Phases Data System (MPDS), Switzerland & National Institute for Materials Science (NIMS), Japan, 2016.



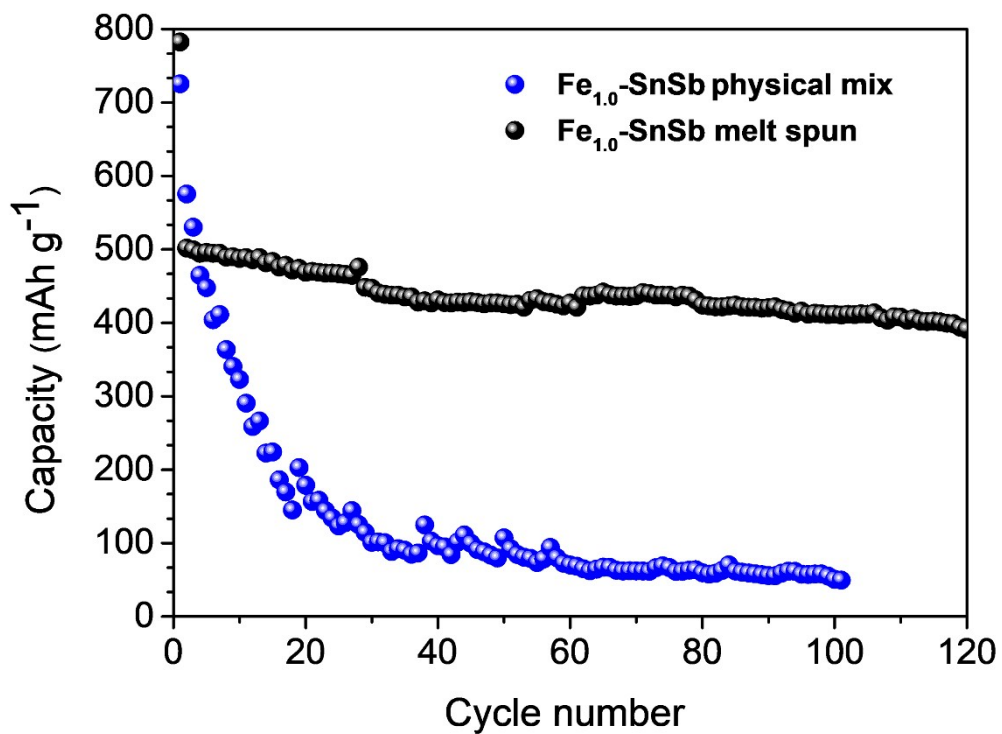
**Figure S5.** XPS analysis of the Fe-Sn-Sb alloys.



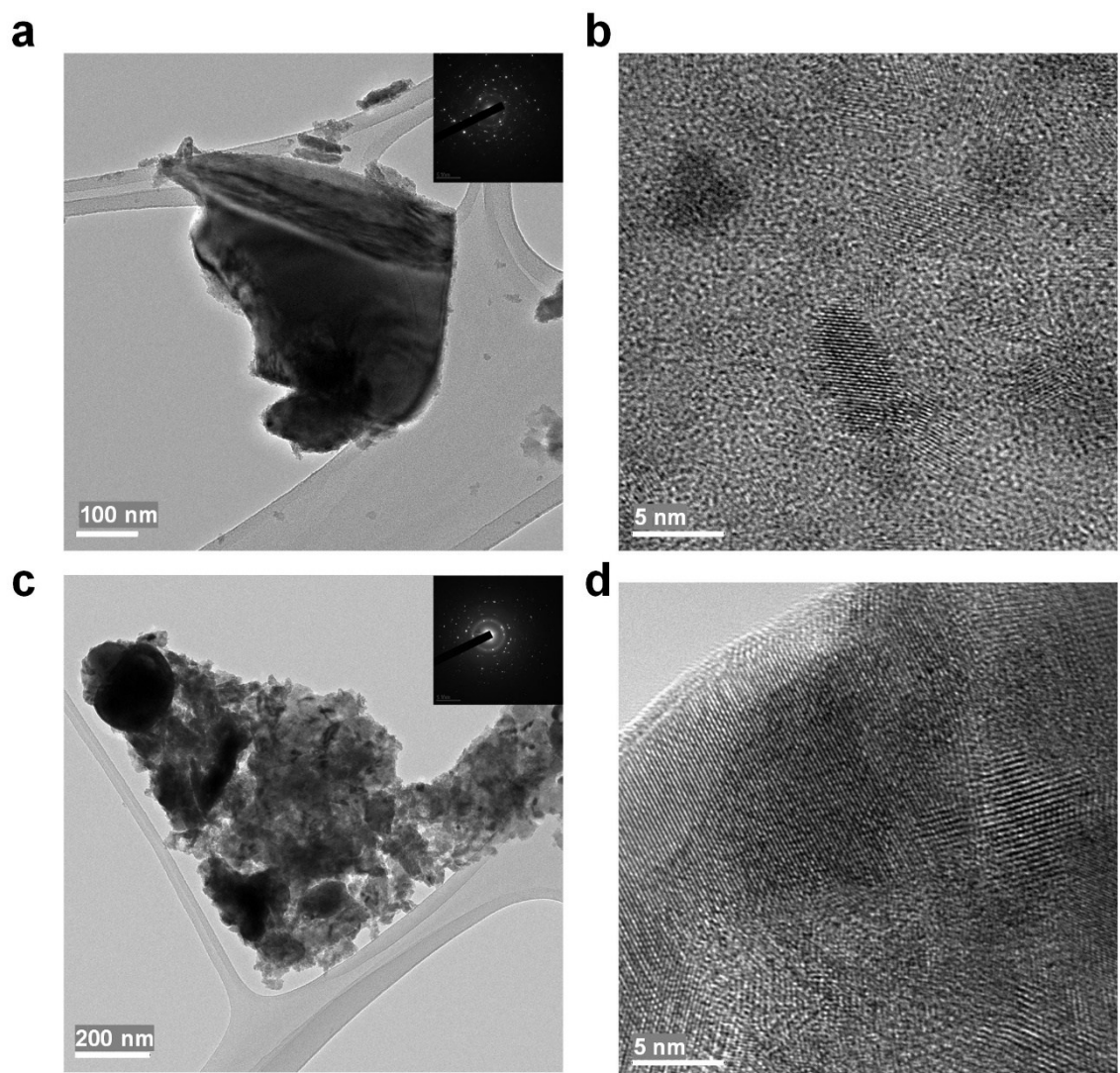
**Figure S6.** Cyclic voltammogram of  $\text{Fe}_{1.0}\text{-SnSb}$  alloy anode.



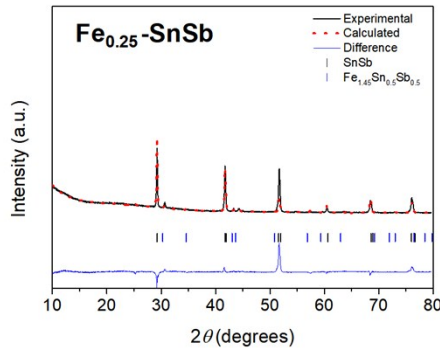
**Figure S7.** Impedance spectra of SnSb and  $\text{Fe}_{1.0}\text{-SnSb}$  anodes.



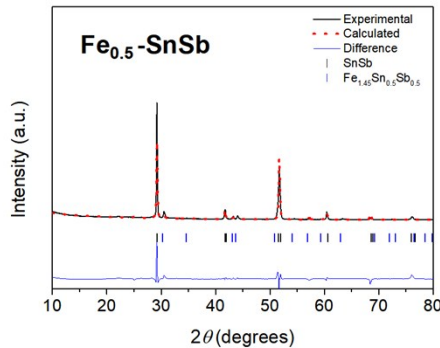
**Figure S8.** Enhanced cycling stability of the rapidly solidified  $\text{Fe}_{1.0}\text{-SnSb}$  alloy against the control sample which is a physical mix of the Fe, Sn and Sb metal powders in the same ratio.



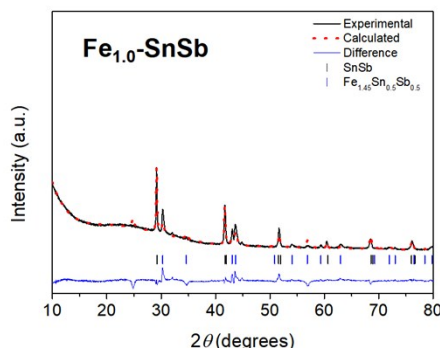
**Figure S9.** HRTEM images of (a, b)  $\text{Fe}_{0.25}\text{-SnSb}$  and (c, d)  $\text{Fe}_{0.5}\text{-SnSb}$  alloys

**a**

Fe <sub>0.25</sub> -SnSb		
SnSb	<i>R-3mR</i> , $a$ (Å) = 6.1396(4), $\alpha$ (°) = 89.9201(4)	93.87 wt.%
Fe <sub>1.45</sub> Sn <sub>0.5</sub> Sb <sub>0.5</sub>	<i>P63/mmc</i> , $a$ (Å) = 4.1013(9), $c$ (Å) = 5.1891(2)	6.13 wt.%

**b**

Fe <sub>0.5</sub> -SnSb		
SnSb	<i>R-3mR</i> , $a$ (Å) = 6.1410(1), $\alpha$ (°) = 90.0004(4)	80.69 wt.%
Fe <sub>1.45</sub> Sn <sub>0.5</sub> Sb <sub>0.5</sub>	<i>P63/mmc</i> , $a$ (Å) = 4.1216(7), $c$ (Å) = 5.1905(4)	19.31 wt.%

**c**

Fe <sub>1.0</sub> -SnSb		
SnSb	<i>R-3mR</i> , $a$ (Å) = 6.1279(2), $\alpha$ (°) = 89.8916(4)	66.34 wt.%
Fe <sub>1.45</sub> Sn <sub>0.5</sub> Sb <sub>0.5</sub>	<i>P63/mmc</i> , $a$ (Å) = 4.1423(2), $c$ (Å) = 5.1802(4)	33.66 wt.%

**Figure S10.** Rietveld refined quantitative phase analysis of Fe-Sn-Sb alloy.

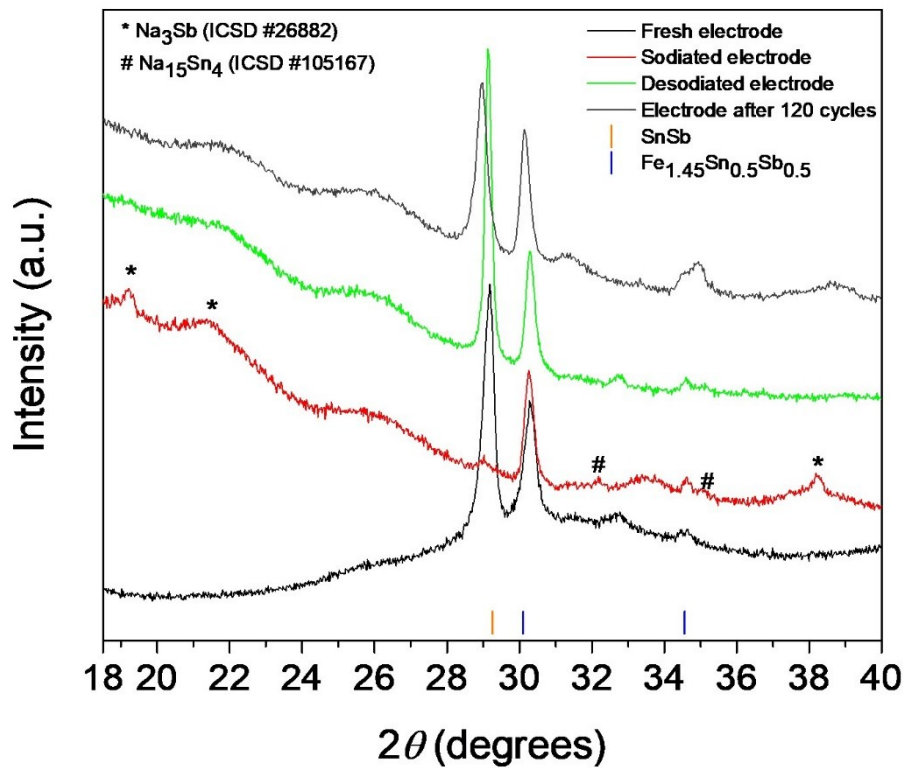


**Figure S11.** *Ex situ* XRD of  $\text{Fe}_{1.0}\text{-SnSb}$  anode at various stages of cycling.

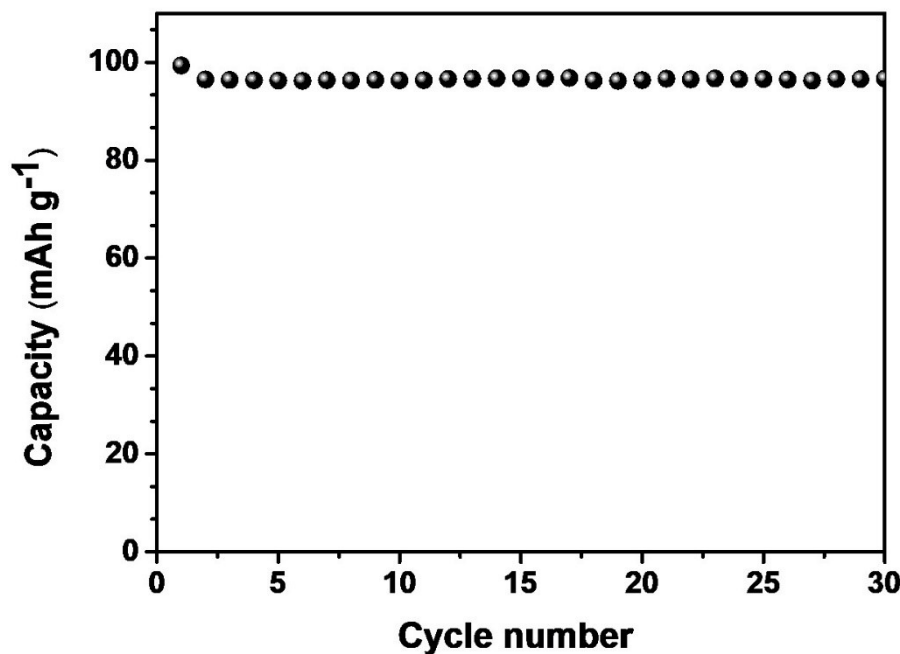


**Figure S12.** Galvanostatic cycling performance of  $\text{NaVPO}_4\text{F}/\text{Na}$  half-cell at a specific current of  $50 \text{ mA g}^{-1}$  in the potential window 2-3.8 vs.  $\text{Na}^+/\text{Na}$ .

**Table S1.** Rietveld-refined lattice parameters of rapidly solidified SnSb alloy

<b>Structural formula</b>	SnSb
<b>Space group</b>	$R\text{-}3mR$
<b>Crystal system</b>	Trigonal
<b>Refined lattice parameters</b>	$a=b=c=6.136 \text{ \AA}$ $\alpha=\beta=\gamma=89.725^\circ$
<b>R-values</b>	$R_{\text{Bragg}}=3.411$ ; $R_{\text{wp}}=5.62$ ; $R_{\text{p}}=3.52$
<b>Crystallite size Lorentzian (nm)</b>	88.4

**Table S2.** Comparison of electrochemical performance of recently reported SnSb anodes

Material	Synthesis method	Capacity @ Specific current (voltage window vs. Na)	Cycles	Reference
<b>SnSb nanoparticles@3D-carbon matrix</b>	<i>Freeze-drying assisted solid-state method</i>	$\sim 350 \text{ mAh g}^{-1}$ @ $0.1 \text{ A g}^{-1}$ (0.01-2 V)	100	2
<b>Porous SnSb</b>	<i>Melt spinning and etching</i>	$\sim 450 \text{ mAh g}^{-1}$ @ $0.05 \text{ A g}^{-1}$ (0.005-2 V)	100	3
<b>Reduced graphene oxide incorporated SnSb@Carbon nanofiber matrix</b>	<i>Electrospinning</i>	$\sim 490 \text{ mAh g}^{-1}$ @ (0.01-2.5 V)	200	4
<b>SnSb@3D N-doped porous graphene</b>	<i>Spray pyrolysis</i>	$\sim 450 \text{ mAh g}^{-1}$ @ $0.1 \text{ A g}^{-1}$ (0.005-3 V)	100	5
<b>SnSb@reduced graphene oxide@carbon microfibers</b>	<i>Centrifugal spinning</i>	$\sim 350 \text{ mAh g}^{-1}$ @ $0.05 \text{ A g}^{-1}$ (0.01-2.5)	200	6
<b>Fe-Sn-Sb alloy</b>	<i>Rapid-solidification/Melt spinning</i>	$\sim 500 \text{ mAh g}^{-1}$ @ $0.05 \text{ A g}^{-1}$ (0.005-2 V)	120	<b>This work</b>

## References

1. Fe-Sb-Sn Isothermal Section of Ternary Phase Diagram: Datasheet from "PAULING FILE Multinaries Edition – 2012" in SpringerMaterials [https://materials.springer.com/isp/phase-diagram/docs/c\\_0203023](https://materials.springer.com/isp/phase-diagram/docs/c_0203023)).
2. W. Wang, L. Shi and Q. Li, *Journal of The Electrochemical Society*, 2018, **165**, A1455-A1459.
3. J.-H. Choi, C.-W. Ha, H.-Y. Choi, J.-W. Seong, C.-M. Park and S.-M. Lee, *Journal of Power Sources*, 2018, **386**, 34-39.
4. H. Jia, M. Dirican, C. Chen, J. Zhu, P. Zhu, C. Yan, Y. Li, X. Dong, J. Guo and X. Zhang, *ACS Applied Materials & Interfaces*, 2018, **10**, 9696-9703.
5. J. Qin, T. Wang, D. Liu, E. Liu, N. Zhao, C. Shi, F. He, L. Ma and C. He, *Advanced Materials*, 2018, **30**, 1704670.
6. H. Jia, M. Dirican, J. Zhu, C. Chen, C. Yan, P. Zhu, Y. Li, J. Guo, Y. Caydamli and X. Zhang, *Journal of Alloys and Compounds*, 2018, **752**, 296-302.